Study of Exotic Nuclei

A Summary of the Thesis Submitted
to the

University of Allahabad
for the degree of

Doctor of Philosophy
in Science

by

Praveen Chandra Srivastava

Under the Supervision of

Prof. (Mrs.) Indira Mehrotra
Head, Physics Department
University of Allahabad
Allahabad -211002
INDIA

Year 2009

"The shell model, although proposed by theoreticians, really corresponds to the experimentalist's approach"

M. Goeppert-Mayer, Nobel Lecture, 12th December 1963

Exotic nuclei refer to β-unstable nuclei with extreme ratios of proton to neutron number on both the proton and the neutron rich sides of stability. In order to form a stable atomic nucleus an equilibrium between the number of protons and neutrons has to be maintained. This condition is fulfilled for 259 different combinations of protons and neutrons and these nuclei can be found on Earth. In addition 26 nuclei form a quasi-stable configuration, i.e. they decay with a half-life comparable to or longer than the age of the Earth and therefore are still present on Earth. In addition to these 285 stable or quasi-stable nuclei, some 4000-6000 unstable nuclei are predicted to exist by different models. Close to 2500 nuclei have been observed already and rest are still in *terra incognita*.

Exotic nuclei can be produced in nuclear reactions induced by Radioactive Nuclear Beams (RNB). After production the nuclei of interest are usually separated electromagnetically from the other reaction products before they can be studied. Such studies have led to the discovery of some new phenomena like halo, skin formation, proton radioactivity, the melting of shell structure at existing magic numbers and appearence of new magic numbers.

The modern large-scale shell-model calculations give at present the most accurate and comprehensive description of nuclei including those at very neutron-rich or very proton-rich edges. It can not only predict low-lying levels but can also make theoretical predictions for comparison with the experimental data like g-factor, magnetic moments and quadrupole moments of very exotic nuclei. The success of this approach is firstly the use of large valence spaces that contain the most relevant degrees of freedom of the problem. For this new shell model codes like ANTOINE and NATHAN from Strasbourg group [Cau89] [Cau99] using Cluster computer and the new approximate methods of solving the nuclear secular problem such as the quantum Monte Carlo diagonalization method put forward by the Tokyo group have been instrumental in achieving this goal. The second is the improvement in our mastering of the effective "in-medium" nuclear interaction to be used in large valence spaces. This comes mainly from the work of A. Zuker and collaborators [Duf96] who have shown that the multipole part of the interaction-responsible for the mixing and the correlations (pairing, quadrupole etc.)-is nearly universal.

Besides, the effective interactions obtained from G-matrices produce it correctly. The monopole part gives the skeleton upon which the coherent multipole terms build the structure of the nucleus. Other recent shell model studies of exotic nuclei include the Caltech Oak Ridge shell model Monte Carlo calculations [Dea99] using effective interactions from Oslo group [Jen95] and the work of MSU group [Bro01].

In the present work, we have performed large scale shell model calculations for exotic nuclei falling in different regions of nuclear chart. The calculations have been performed with different types of effective interactions for each set of nuclei.

The aim of the present work is to

1. test the suitablity of chosen valence spaces and effective interactions for different nuclei over nuclear chart in explaning the experimental data.

2. to compare the predicted values of nuclear properties with the experimental data wherever available.

3. to make predictions for the unknown energy levels and transition rates which can serve as basis for future experiments.

4. to study the variation in the shell structure in nutron rich nuclei in moving from magic number N=8 to N=50.

5. to design an effective interaction for the *fpg* shell which can account for the experimental data for neutron rich Ni, Cu and Zn isotopes.

The thesis comprises of following eight chapters: **Chapter 1** -Exotic Nuclei; **Chapter 2** - Shell model and techniques of calculation; **Chapter 3**-Shell model study of neutron rich oxygen and fluorine isotopes; **Chapter 4**-Large scale shell model calculations for $^{61-66}$Fe isotopes; **Chapter 5**-Large scale shell model calculations for odd-odd $^{58-62}$Mn isotopes; **Chapter 6**-Large scale shell model calculations in Ni region: ^{56}Ni as a core; **Chapter 7**- Large scale shell model calculations in Ni region: ^{40}Ca as a core; **Chapter 8**-Conclusions and future prospects.

Chapter 1, in this chapter exotic nuclei and world wide radioactive nuclear beam facilities are discussed. The special features of exotic nuclei, such as neutron halo, skin and proton radioactivity phenomena are also discussed in brief. In the present work nuclear structure studies have been carried out for neutron rich exotic nuclei in three regions of nuclear chart. These are neutron rich isotopes of O and F up to A=29 (sd shell), of Fe up to A=66 and Mn up to A=62 (fp shell) and of Ni, Cu and Zn up to A=80 (fpg shell). Experimental data on the energy levels of neutron

rich isotopes of O and F have recently been made available up to A=29 using the technique of β-dalayed γ-ray spectroscopy [Mic06][NNDC]. Recently at Legnaro National Laboratories neutron rich Fe isotopes were populated through multinucleon transfer reaction by bombarding a ^{238}U target with ^{64}Ni beam [Lur07]. Analysis of the gamma spectrum of neutron rich Fe isotopes has provided data on their level structures. Experimental data on the neutron rich Mn isotopes from A= 59-63 has been made available by Valiente-Dobón *et al.* [Dob08] through mutineutron transfer reaction on ^{238}U target with 460 MeV ^{70}Zn beam. The first identification of $^{70-74}$Ni and lifetime determination of $^{71-74}$Ni have been carried out through thermal-neutron-induced fission of ^{235}U and ^{239}Pu at Lohengrin recoil spectrometer of ILL-Grenoble [Ber90]. The neutron-rich isotopes $^{68-74}$Ni have been recently produced at the LISOL-Leuven facility in the fission of ^{238}U induced by a 30-MeV proton beam [Fra01]. All these recent available experimental data have motivated to undertake theoretical study of the above mentioned nuclei. All calculations have been performed in the framework of nuclear shell model. The properties calculated are energy levels, wavefunctions, transition rates and quadrupole moments. Two important features of exotic nuclei have been reported in the literature. First is the melting of traditional magic numbers and appearance of new numbers. Second is the variation of single particle energy levels of proton as more and more neutrons are added to the isotopes - the so called 'monopole shift'. In going from $^{17}_{8}O_9$ to $^{76}_{28}Ni_{48}$, the magic numbers from Z and or N = 8 to 50 is covered. Similarly the N/Z ratio is covered from 1.21 to 1.71. The above two features have been studied in detail for the isotopes considered in the present work.

Chapter 2, gives a brief account of nuclear shell model. The standard phenomenological mean field potential is given by harmonic oscillator with additional term $\alpha\ \vec{l}.\vec{s}$ and $\beta\ \vec{l}.\vec{l}$. This potential can explain the known magic numbers characterized by large binding energy and extra stability. In the microscopic approach the mean field is obtained from the nucleon-nucleon interaction potential by "self-consistent" Hartree-Fock method. The nuclear shell model is one of the main theoretical tools for understanding the properties of nuclei. The configuration mixing calculations are performed in limited configuration space. The neglected configurations tend to renormalize the bare nucleon-nucleon interaction potential. The effective interactions so generated can be classified in three categories: microscopic, phenomenological and schematic interaction. The three pillars of the shell model are namely, valence space, effective interaction and shell model code to diagonalize the matrices. Two main problems arise in a shell model description of the nuclear struc-

ture. The first one is to obtain a renormalized effective interaction in a given valence space from the bare nucleon-nucleon force. The second problem is that with increase of the size of the valence space or the increases in the number of particles (holes) the dimension of matrices explodes. In this chapter two codes used in the present work have been discussed. The Nushell is a shell model code developed by Alex Brown from MSU to tackle dimensions up to 10^6 in the J-T scheme and about 2×10^7 in the M-scheme. Nushell generates the basis states in m-scheme and then computes the matrix in the j scheme. Therefore, it bypasses the complication of the angular momentum algebra in j-j coupled basis and also avoids the huge matrix dimension generated during m-scheme. Nushell consists of seven main programs and some supporting codes. SHELL makes a batch file .*bat that coordinates the program sequence and their inputs. NUBASIS makes a list of all possible M-scheme basis states for a given model space together with a given set of restrictions. NUPROJ makes linear combinations of the M-scheme basis states that have good J values in p/n formalism or good J and T in isospin formalism. NUMATRIX makes the matrix corresponding to the J (or JT) dimension of the problem. NULANCZOS find the lowest N eigen values for the matrix. MVEC reads the output of Proj and Lanczos to make the eigenvectors in the M-scheme basis. TRAMP calculates overlaps between two wavefunctions. DENS calculates the radial wavefunctions for a given nucleus with oscillator, Woods-Saxon or skyrme Hartree-Fock potentials and reads the .*obd from nushell to calculate B(EL), B(ML) and B(GT) values. The shell model code ANTOINE (Caurier and Nowacki, 1999) is based on m-scheme. In the standard diagonalization methods the CPU time increses as N^3, N being the dimension of the matrix. Therefore these methods cannot be used in large-scale shell model calculations. Since, in general, only a few eigenvalues and eigenvectors are needed the iteractive methods are of general use in particular the Lanczos method (Lanczos, 1950).

In **Chapter 3**, results for the shell model study of neuton-rich oxygen and fluorine isotopes have been presented. The neutron-rich oxygen and fluorine isotopes in the vicinity of ^{16}O are currently at the focus of nuclear physics and astrophysics studies. In this region exotic phenomena have been observed, such as the new magic numbers at N=16 [Oza05], the sudden change in the neutron drip line from Z=8 to Z=9 [Sak99] and nuclear deformation region in spite of N=20, i.e., the so called island-of inversion region [War90]. The ground state properties of the neutron-rich oxygen isotopes have been studied using different methods like, large basis shell model approach [Ots99], Hartree-Fock (SHF) approach using skyrme in-

teraction [She96], and relativistic mean-field(RMF) theory [Ren95]. In most of the models [Hau88] nuclear stability is expected for the heavy ^{26}O isotope, while the doubly-magic ^{28}O is predicted unbound against two-neutron emission with two neutron separation energy S_{2n} as 1.3 MeV . Contrary to this experiments at GANIL, MSU and RIKEN show that both ^{26}O and ^{28}O are particle unstable. Double magicity in the neutron-rich ^{22}O with Z=8 and N=14 has been already studied [Bec05]. In the present calculation four different types of interactions are used. The first set of shell model calculations (SM-I) utilises phenomanological Preedom-Wildenthal interaction [Pre72], the second set of shell model calculations (SM-II) utilises Wildenthal-Mcgrory modified surface delta interaction interaction [Wil71], the third set of shell model calculation (SM-III) is semi-empirical interaction named as SDPOTA interaction and the fouth set of shell model calculation(SM-IV) is renormalised Kuo interaction [Kuo67]. Preedom Wildenthal (PW) interaction has been obtained by empirically modifying some of the matrix elements of Kuo interaction in order to achieve an rms best fit between observed energies of 72 levels in A=18-22 region. The single-particle energies are taken from ^{17}O spectrum. Wildenthal-Mcgrory modified surface delta interaction is the surface delta interaction (SDI) to which an isospin dependent monopole term is added. The MSDI is expresed as

$$V_T(ij) = -4\pi A_T \delta(r_i - r_j) f_{ij} + B_T$$

The main advantage of using MSDI interaction is that in the parameterization technique, the 63 TBME of sd shell Hamiltonian are specified by 4 parameters together with three single particle energies. This leads to a total of 7 parameters to specify the complete Hamiltonian. Optimized values of these 7 parameters were obtained by the best fit of 11 ground state and 55 excitation energies of nuclei with A=30-34. SDPOTA interacion is a semi-empirical best-fit interaction based on a 14-parameter density-dependent two-body potential. The results of our calculation for the energy levels of neutron rich oxygen isotopes $^{20-26}$O are shown for four different interactions. The results are shown upto maximum of $J^\pi=4^+$ for even isotopes and $J^\pi=9/2^+$ for odd isotopes and for the first two(one) states for each spin and parity. The experimental results upto 6-7 MeV excitation energies are known for ^{20}O,^{21}O and ^{22}O. For ^{23}O and ^{25}O only ground state J^π is known. No experimental data is available for ^{24}O and ^{26}O. It is observed that in even O isotopes the spin and parity of the ground state and the first excited state is correctly reproduced in all the cases. In ^{20}O correct ordering is also reproduced for the first two interactions. For ^{21}O ground state J^π is correctly predicted for all the interactions except for SDPOTA. The $3/2^+$ state predicted above the first $1/2^+$ state in all the theoretical calculations

is missing in the experimental data. The ordering of the remaining from experimentally observed levels is correctly reproduced except for SDPOTA. The ground state J^π for ^{23}O and ^{25}O is correctly reproduced for all the interactions. The variation of excitation energy of first excited 2^+ state for even-even O isotopes has been studied as a function of the neutron number N. The large excitation energy of the first 2^+ excited state for N=16 followed by decline in its value for neighbouring isotopes is an indication of shell closer at N=16. This is supported by small value of B(E2) transition rate and also of quadrupole moment for this isotope. Earlier studies have suggested shell closer at N=14 and N=16. However in our calculations features of shell closer at N=14 are not indicated.

In F isotopes a valence proton in j_π orbital interacts with a number of valence neutron particles filling a set of neutron orbitals j_ν.
The Hamiltonian can be written as

$$\hat{H} = \epsilon_{j_\pi} + \sum_{j\nu} \epsilon_{j_\nu} \hat{n}_{j_\nu} + V_{\pi\nu} \tag{1}$$

where ϵ_{j_π} and ϵ_{j_ν} denotes the single particle energies of proton and neutron corresponding to states j_π and j_ν respectively, n_{j_ν} is the number operator for neutrons occupying state j_ν and $V_{\pi\nu}$ represents the residual proton-neutron interaction. The neutron-neutron interactions within the valence neutron space have been neglected.

If $V_{\pi\nu}$ interaction is decomposed into different multipoles, $\hat{H}$ can be written as

$$\hat{H} = \hat{H}_{\lambda=0} + higher\ \lambda\ multiples\ of\ \pi\nu\ interaction \tag{2}$$

where the monopole Hamiltonian $\hat{H}_{\lambda=0}$ is given by

$$\hat{H}_{\lambda=0} = \sum_{j\pi} \tilde{\epsilon}_{j_\pi} \hat{n}_{j_\pi} + \sum_{j\nu} \tilde{\epsilon}_{j_\nu} \hat{n}_{j_\nu} \tag{3}$$

and $\tilde{\epsilon}_{j_\pi}$ is the monopole corrected single particle proton energy which is given by

$$\tilde{\epsilon}_{j_\pi} = \epsilon_{j_\pi} + \sum_{j\nu} \bar{E}(j_\pi j_\nu) \hat{n}_{j_\nu} \tag{4}$$

The operator $\hat{n}_{j_\nu}$ in Eq.(4) is replaced by its expectation value $\langle \hat{n}_{j_\nu} \rangle = \hat{n}_{j_\nu}$, the number of neutrons occupying orbital j_ν [Sha63, Hey94, Law80].

The term $\bar{E}(j_\pi j_\nu)$ is angular momentum averaged interaction energy

$$\bar{E}(j_\pi j_\nu) = \frac{\sum_j (2J+1) \langle j_\nu j_\pi; J \mid V \mid j_\nu j_\pi; J \rangle}{\sum_j (2J+1)} \tag{5}$$

The monopole energy shift for the proton orbital in $^{19-29}$F isotopes have been studied as a function of changing neutron number (N) for four different interactions. The variation of ESPEs for these interactions point out towards appearance of shell closer at N=14 and its disappearance at N=16.

In **Chapter 4**, large scale shell model calculations for $^{61-66}$Fe isotopes have been studied. In the present work we have performed large scale shell model calculations on neutron rich $^{62-66}$Fe isotopes with GXPF1A interaction without any truncation. The calculations have been carried out in valence space of full *fp* shell consisting of $0f_{7/2}$, $1p_{3/2}$, $0f_{5/2}$ and $1p_{1/2}$ orbitals and treating ^{40}Ca as the inert core. No restriction has been put on the number of particles which can be excited to higher level. The aim of this work is to test the suitability of GXPF1A interaction towards the end of *fp* shell. Also by comparing the results of present work with that of Ref [Lur07] one can get some insight on the role of $g_{9/2}$ orbit in explaining the data. The configuration space for valence particles is taken as full *fp* shell which is made up of all Pauli allowed combinations of valence particles in the $0f_{7/2}$, $1p_{3/2}$, $0f_{5/2}$, and $1p_{1/2}$ orbitals for both the protons and the neutrons. The calculations have been performed at the SGI-cluster computer at GANIL with the code `ANTOINE` [Cau89] [Cau99]. In this code the problem of giant matrices is solved by splitting the valence space into two parts, one for the proton and another for the neutron. The states of the basis are written as the product of two Slater determinants (SD), one for protons and another for neutrons: $\mid I\rangle = \mid i, \alpha\rangle$ (Here capital letter refers to full space and lower case letters refer to subspaces of proton and neutron). The Slater determinants i and α can be classified by their M values, M_1 and M_2. The total M being fixed, the SD of the two subspaces will be associated only if $M_1 + M_2 = M$. The calculated energy levels obtained with GXPF1A interaction for even Fe isotopes are compared with the experimental data and also with the results obtained with '*fpg*' interaction in a truncated configuration space. It is observed that large scale shell model calculations with GXPF1A interaction in full *fp* space gives very good agreement with the experimental data for ^{62}Fe. For 2^+, 4^+ and 6^+ states of ^{62}Fe the discrepancies with experimental data are 70, 5 and 138 KeV respectively whereas with '*fpg*' interaction the corresponding values are 6, 219 and 494 KeV. But the discrepancy with the experimental data increases as we go towards N=40. The '*fpg*' interaction with truncation on the number of particles getting excited gives better result. This shows the importance of $g_{9/2}$ orbital in explaining the data for A=66. This can be understood in terms of decrease in the energy gap between *fp* shell and $g_{9/2}$ orbital in going towards N=40 and can be attributed to the proton neutron

monopole tensor interaction [Hon04]. Thus the recent data on ^{62}Fe can be explained very well in the framework of large scale shell model calculations with GXPF1A interaction in full *fp* space with no truncation without including $0g_{9/2}$ orbital. The fit is reasonably satisfactory for ^{64}Fe, but agreement with the experimental data on ^{66}Fe is not good. The most dominant contribution in the ground state of ^{62}Fe is $(0f_{7/2})^8$, $(1p_{3/2})^4$, $(1p_{1/2})^0$ and $(0f_{5/2})^4$ whereas that of ^{64}Fe is $(0f_{7/2})^8$, $(1p_{3/2})^4$, $(1p_{1/2})^2$ and $(0f_{5/2})^4$ indicating the change in the ordering of $1p_{1/2}$ and $0f_{5/2}$ levels.

It is observed that negative parity states of ^{61}Fe can be well reproduced with GXPF1A interaction in full *fp* space without truncation. For ^{63}Fe the correct ordering of levels is not reproduced. The structure of the wave function for the ground state and the first excited state suggest that the orderings of the single particle energy levels gets modified due to monopole correction. The results of our calculation obtained with GXPF1A interaction for ^{61}Fe and ^{63}Fe isotopes are compared with the experimental data and also with the results of Lurandi *et al*. obtained with *fpg* interaction in a truncated configuration space [Lur07]. In the case of ^{61}Fe the calculated energy difference between $1/2^-$ and $3/2^-$ is only of the order of 86 KeV. If this difference being less than 100 KeV neglected, the ordering of the levels is correctly reproduced. For *fpg* interaction also $1/2^-$ level lies 36 KeV below $3/2^-$ level and has been suppressed in the figure (Lurandi *et al*. private communication). The calculated $7/2^-$ state is at 988 KeV above the ground state compared to the experimental value of 959 KeV. In the case of ^{63}Fe measured ground state spin is $5/2^-$ and the first excited $3/2^-$ state lies above 356 KeV. GXPF1A interaction predicts ground state spin as $3/2^-$ after suppresing $1/2^-$. The same is true for *fpg* interaction. The first excited state is at 298 KeV with spin $5/2^-$ and next state is at 1152 KeV with spin $5/2^-$. The $\epsilon_{5/2^-} \sim \epsilon_{3/2^-}$ energy difference is 298 KeV for GXPF1A interaction and 192 KeV for *fpg* interaction compared to the experimental value of 356 KeV. In going from ^{61}Fe to ^{63}Fe for the ground state the occupancy of $1p_{1/2}$ level rises from 0 to 1 and that of $0f_{5/2}$ level from 3 to 4. In the most dominant configuration for the ground state in ^{61}Fe, $1p_{1/2}$ level is unoccupied and $0f_{5/2}$ level is relatively more important. In the ground state of ^{63}Fe, $1p_{1/2}$ state is only partially occupied. In the case of ^{63}Fe the ground state spin and the correct ordering of the energy levels is not predicted with GXPF1A interaction as also was the case with *fpg* interaction. The wave function structure shown in table indicates preferred filling of $0f_{5/2}$ levels over the $1p_{1/2}$ level. This indicates that the single particle energy levels get renormalized due to the monopole effect. These attractive and repulsive interactions affect cooperatively the single particle energies and may change the ordering of lev-

els. The results of our calculations show that in ^{61}Fe the levels are well reproduced with GXPF1A interaction and for lower levels the agreement is better than that with *fpg* interaction. This indicates that full *fp* space is sufficient for explaining the negative parity states of ^{61}Fe and inclusion of $0g_{9/2}$ is not important. The ground state spin and the ordering of the two experimentally known levels of ^{63}Fe has not been correctly reproduced for both the interactions. The ground state spin of ^{63}Fe can be explained as arising from the $\nu(0f_{5/2})\otimes 0^+(^{62}\text{Fe})$ configuration. The structure of wave functions for these isotopes suggest that single particle energy levels get modified due to monopole interaction which plays a decisive role in filling the levels.

In **Chapter 5**, large scale shell model calculations have been carried out for odd-odd $^{58-62}$Mn isotopes in two different model spaces. First set of calculations have been carried out in full *fp* shell valence space with two recently derived *fp* shell interactions namely GXPF1A and KB3G treating ^{40}Ca as core. The second set of calculations have been performed in *fpg* valence space with the *fpg* interaction treating ^{48}Ca as core and imposing truncation on the number of valence particles. Correct ordering of ground state and the first excited state levels for ^{58}Mn is predicted only with *fpg* interaction showing the importance of $0g_{9/2}$ orbital in the valence space for this nucleus. None of the interactions could predict the correct ordering of levels for ^{62}Mn. Experimental data on ^{62}Mn is sparse. More experimental data and location of negative parity states is needed to ascertain the importance of $0g_{9/2}$ and higher orbitals in interpreting the experimental data. For *fp* valence space the GXPF1A and KB3G interactions have been used. For more neutron rich Mn isotopes it is necessary to include $g_{9/2}$ orbital from *sdg* shell. Thus we have used *fpg* interaction to compare the results with experimental findings. The configuration space for GXPF1A and KB3G interaction is taken as full *fp* shell which is made up of all Pauli allowed combinations of valence particles in the $0f_{7/2}$, $1p_{3/2}$, $0f_{5/2}$ and $1p_{1/2}$ orbitals for both protons and neutrons. The *fpg* model space comprises of the $0f_{7/2}$, $1p_{3/2}$, $0f_{5/2}$, $1p_{1/2}$ active proton orbitals and $0f_{7/2}$, $1p_{3/2}$, $0f_{5/2}$, $1p_{1/2}$, $0g_{9/2}$ neutron orbitals with eight $f_{7/2}$ frozen neutrons. For the *fpg* valence space, an effective interaction was built up [Sor02] using *fp* two-body matrix elements (TBME) from Ref. [Pov01] and $1p_{3/2}$, $0f_{5/2}$, $1p_{1/2}$, $0g_{9/2}$ TBME from Ref. [Now96]. For the common active orbitals in these subspaces, matrix elements were taken from [Now96]. As the latter interaction was defined for a ^{56}Ni core, a scaling factor of $A^{-1/3}$ amplitude was applied to take into account the change of radius between the ^{40}Ca and ^{56}Ni cores. As more and more protons are added in the $f_{7/2}$ shell, the excitation energy of the $9/2^+$ state gets decreased due to the attractive $\pi f_{7/2}\nu g_{9/2}$ interaction. The remaining

matrix elements were taken from $f_{7/2}g_{9/2}$ TBME from Ref. [Kah69]. In *fpg* we used truncation by allowing up to a total of six particle excitations from the $f_{7/2}$ orbital to the upper *fp* orbitals for protons and from the upper neutron *fp* orbitals to the $g_{9/2}$ orbital. The results of earlier calcultions [Lid06] with GXPF1 are also shown for comparison. GXPF1A and KB3G interactions predict the ground state spin as 4^+ and 1^+ state lies at 41 KeV and at 11 KeV above the ground state respectively. *fpg* interaction gives the correct ground state spin 1^+ as also obtained experimentally. The first 4^+ excited state is predicted at about 26 KeV against the experimental value of 71 KeV. It is observed that in going from GXPF1 to GXPF1A and then to KB3G the predicted energy difference between the first excited 1^+ state and the 4^+ ground state decreses from 72 to 41 and then to 11 KeV. Finally when the $g_{9/2}$ orbital is included in the valence space, the 1^+ state comes below 4^+ state as observed experimentally. This shows the importance of $g_{9/2}$ orbital in the valence space. The experimental data predicts 5^+ level at 448 KeV and 2^+ level at 1325 KeV. There are six 1^+ states other than ground state and three levels with unassigned spin. In our calculation a 5^+ level is predicted at 386 KeV for GXPF1A, 471 KeV for KB3G and 616 KeV for *fpg*. The first predicted 2^+ level lies around 145 KeV and may correspond to observed experimental value of 160 KeV with unassigned spin. The second 2^+ level is predicted at 168 KeV for GXPF1A, 379 KeV for KB3G and 446 KeV for *fpg*. The number of predicted 1^+ levels below 2 MeV is two for GXPF1A, two for KB3G and three for *fpg* interaction. The experimental and theoretical low-lying states up to 1.6 MeV for ^{60}Mn are listed. In figure we have shown the comparison of experimental values with those predicted for three different interactions. The ground state spins $J^\pi = 1^+$ is correctly reproduced by GXPF1A and KB3G interaction. The Calculated 4^+ state is at 228 KeV for GXPF1A and at 223 KeV for KB3G compared to the experimental value of 271 KeV. Two states with spin 2^+ and 3^+ have been predicted to lie between 1^+ and 4^+ state for GXPF1A. For KB3G these states lie higher than 2^+. It is observed that *fpg* interaction does not predict correct ground state spin. Experimentally for ^{62}Mn there is an uncertanity in assigning the ground state spin to be 1^+, 3^+ or 4^+. All the calculated results show 2^+ level as the ground state showing the inadequacy of the used valence space. These results indicate that inclusion of $g_{9/2}$ orbital from *sdg* shell is important for increasing N and Z.

In **Chapter 6**, large scale shell model calculations have been performed for neutron rich nickel, copper and zinc isotopes with $40 \leq N \leq 50$ using ^{56}Ni as a core. The calculations have been performed using $p_{3/2}$, $f_{5/2}$, $p_{1/2}$ and $g_{9/2}$ valence space taking ^{56}Ni as a core. In the present calculation we use two different sets of interactions.

The first set of large scale shell model calculations (labeled LSSMI) utilizes the realistic effective nucleon-nucleon interaction based on G-matrix theory by Hjorth-Jensen [Jen95] with the monopole modification by Nowacki [Now96, Smi04]. The second set of calculations (labeled LSSMII) are obtained with the JJ4B effective interaction [Lis04] which is an extension of the renormalized G-matrix interaction based on the Bonn-C *NN* potential (JJ4APN) constructed to reproduce the experimental data for exotic Ni, Cu, Zn, Ge and *N=50* isotones in the vicinity of ^{78}Ni.

For $^{69-73}$Cu, ground state spin is correctly predicted but other Yrast levels are slightly higher in energy in comparison to the experimental value. For $^{75-77}$Cu, predicted ground state spin is $3/2^-$ whereas the experimental value is $5/2^-$. For ^{79}Cu predicted spin of $5/2^-$ agrees with experimental value. The LSSMII calculations predict correct ground state for all the $^{69-79}$Cu isotopes. For ^{69}Cu and ^{71}Cu isotopes Yrast levels are compressed compared to the experimental value. For ^{71}Cu only first $5/2^-$ is lower in energy in comparison to experimental value, while other levels are higher in energy in comparison to experimental values. It is observed that in going from ^{69}Cu to ^{79}Cu as the neutron number increases the first $5/2^-$ gets lower and lower in energy and becomes the ground state for ^{75}Cu onwards. It is observed that in going from ^{69}Cu to ^{73}Cu energy gap between the first excited $5/2^-$ state and $3/2^-$ ground state decreases in energy. For ^{75}Cu the two levels cross each other and $5/2^-$ state becomes the ground state. For ^{70}Ni both interactions predict slightly higher energy of the first 2^+ state. LSSMI and LSSMII predict 2^+ state above the experimental value by 406 KeV and 172 KeV. As the number of neutrons increases from ^{72}Ni onwards both the interactions predict higher levels nearly 500 KeV higher than experimental values. Thus both these interactions fail to reproduce the experimental data of more neutron rich Ni isotopes. The E(4_1^+) energy is well predicted by LSSMI and E(2_1^+) by LSSMII. The high value of E(2_1^+) at N=40 is a clear indication of shell closure. For ^{70}Zn both the interactions predict correct order of levels. The first 2^+ state at 885 KeV are predicted at 997 KeV and at 957 KeV by LSSMI and LSSMII interactions respectively. The LSSMII predicts better results for the first 2^+ state. For ^{72}Zn, the order of levels is correctly reproduced by LSSMII. The 2^+ state is predicted at 302 KeV and 211 KeV above the corresponding experimental values by LSSMI and LSSMII respectively. For ^{74}Zn, 2^+ at 606 KeV is predicted at 879 KeV and at 826 KeV by LSSMI and LSSMII. The results of LSSMII are better than LSSMI. For ^{76}Zn, the 2^+ at 599 KeV is predicted at 840 KeV and at 911 KeV by LSSMI and LSSMII respectively. The 2^+ in ^{78}Zn at 730 KeV is predicted at 1060 and at 1032 KeV and in ^{80}Zn at 1492 KeV is predicted at

1731 KeV and 1353 KeV for LSSMI and LSSMII interactions. Thus as number of neutron increases both these interactions give higher values of 2^+ state in comparison to the corresponding experimental values. The $E(2_1^+)$ is predicted correctly by LSSMI interaction. The higher value of $E(2_1^+)$ at N=50 is a clear indication of shell closure at N=50. B(E2; $2_1^+ \rightarrow 0_{gs}^+$) values for Ni isotopes for different set of effective charges for LSSMI and LSSMII have been computed. The B(E2) for e_π=1.76 and e_ν=0.97 is closer to experimental values in comparison to the other set of values. High values of e_π in both LSSMI and LSSMII are required to reproduce the results indicating a strong Z=28 core polarization. The high experimental B(E2; $2_1^+ \rightarrow 0_{gs}^+$) in ^{70}Ni is not reproduced for both the interactions. This has been interpreted in Ref. [Per06] as a rapid polarization of the proton core induced by the filling of the neutron $1g_{9/2}$ orbit. This reflects a strong monopole interaction between $\pi 1f_{7/2}$-$\nu 1g_{9/2}$. These results show that the dominance of $g_{9/2}$ orbit in B(E2) calculation is important above N=40. B(E2; $2_1^+ \rightarrow 0_{gs}^+$) values for Zn isotopes for different set of effective charges for LSSMI and LSSMII also indicate that higher value of e_π is required to reproduce B(E2) correctly. In Zn isotopes above A=68 the contribution from $\nu 1g_{9/2}^2$ configuration in the wave function of the low lying excited 2_1^+ and 4_1^+ states is important. The B(E2;$2_1^+ \rightarrow 0_{gs}^+$) strength is thus dominated by the specific E2 strength between $(\nu 1g_{9/2})_{J=0}$ and $(\nu 1g_{9/2})_{J=0}$ configurations. The increase of the B(E2) values beyond N=40 suggests an increase of the collectivity induced by the interaction of protons in the pf shell and neutron in the $g_{9/2}$ orbit.

In **Chapter 7**, large scale shell model calculations have been performed for neutron rich nickel, copper and zinc isotopes with $40 \leq N \leq 50$ using ^{40}Ca as a core by including the $f_{7/2}$ orbit. In the previous chapter large scale shell model calculations were performed for neutron rich nickel, copper and zinc isotopes for $40 \leq N \leq 50$ using two different versions [Lis04] [Now96] [Smi04] of effective interactions for the model space consisting of the $p_{3/2}$, $p_{1/2}$, $f_{5/2}$ and $g_{9/2}$. Both, however, yield unsatisfactory results in certain aspects, viz.
(i) large $E(2^+)$ values for very neutron rich nuclei (^{76}Ni and ^{80}Zn),
(ii) small B(E2) values in comparison to experimental values and for
(iii) ^{75}Cu, ^{77}Cu and ^{79}Cu the ground state is $3/2^-$ as compared to the experimental indication of $5/2^-$.

This may be due to neglect of the $f_{7/2}$ orbit for the protons. In view of this $f_{7/2}$ orbit has been included in the valence space of protons by taking ^{40}Ca as a core. Effective interaction for fpg valence space for both protons and neutrons with

^{40}Ca as core has been constructed by Sorlin *et al.* [Sor02]. The main drawback of this interaction is that the effective proton single-particle energies of $f_{7/2}$ orbital become lower than $f_{5/2}$ which is not realistic. In the present work we have modified 28 TBME to account for this discrepancy.

In the present chapter, we have used *fpg* model space comprising of the $0f_{7/2}$, $1p_{3/2}$, $0f_{5/2}$, $1p_{1/2}$ active proton orbitals and $0f_{7/2}$, $1p_{3/2}$, $0f_{5/2}$, $1p_{1/2}$, $0g_{9/2}$ neutron orbitals with eight $f_{7/2}$ frozen neutrons, more accurately ^{40}Ca core with eight $f_{7/2}$ frozen neutrons. For the *fpg* valence space an effective interaction with ^{40}Ca as core has been reported in Ref. [Sor02]. This interaction has been built using *fp* two-body matrix elements (TBME) from Ref. [Pov01] and $1p_{3/2}$, $0f_{5/2}$, $1p_{1/2}$,$0g_{9/2}$ TBME from Ref. [Now96]. For the common active orbitals in these subspaces, matrix elements were taken from [Now96]. The remaining matrix elements are taken from $f_{7/2}g_{9/2}$ TBME from Ref. [Kah69].

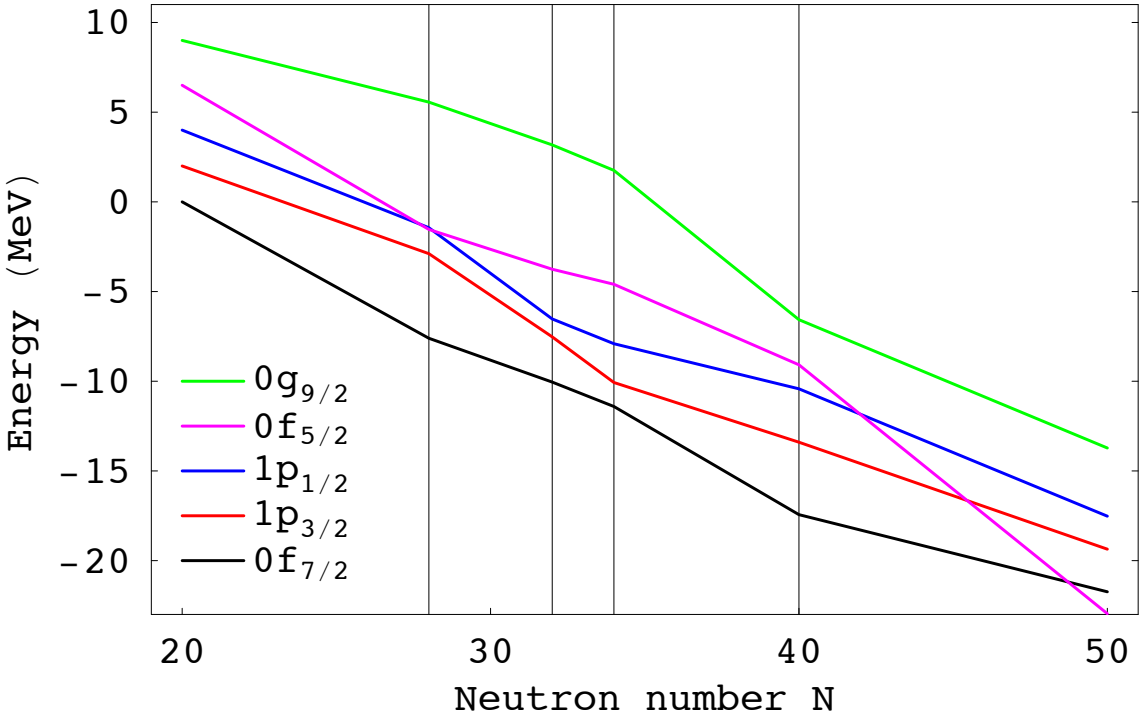

Figure 1: Effective proton single-particle energies in $^{41-71}$Sc isotopes using *pfg9* interaction.

The modefied interaction has been tuned to reproduce the experimental data of Cu isotopes. These being odd nuclei the available experimental data is sparse. The

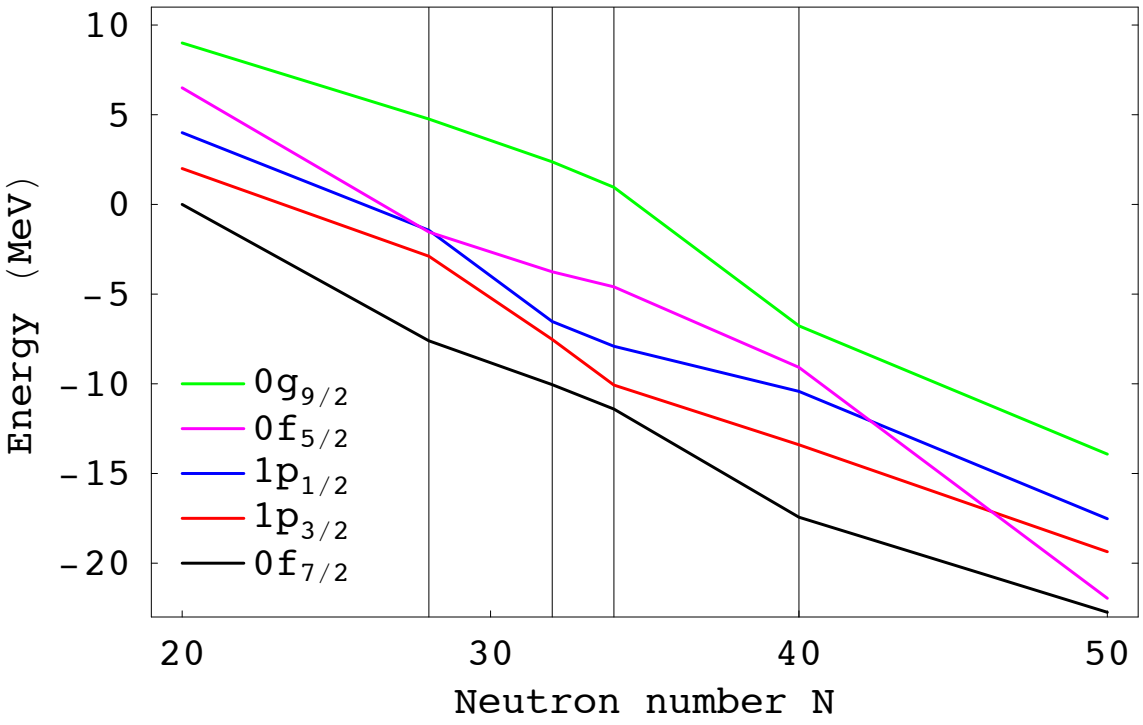

Figure 2: Effective proton single-particle energies in $^{41-71}$Sc isotopes using *pfg9a* interaction.

aim of this tunning is to first reproduce the ground state properties of $^{75-79}$Cu and then apply it to Ni and Zn isotopes. In the original fpg interaction $f_{5/2}$ level crosses the $f_{7/2}$ at ^{70}Sc and becomes lower. This appears to be unrealistic. To correct this $g_{9/2}f_{7/2}$ matrix elements have been changed by subtracting 100 KeV and $g_{9/2}f_{5/2}$ matrix elements by adding 100 KeV from the original TBME of fpg interaction. This modified interaction is renamed as *pfg9a*. The effective proton single particle energy for $f_{7/2}$ in $^{41-71}$Sc isotopes is always lower than $f_{5/2}$ which as an expected.

Since the dimension of matrices involved for pfg9/2 space is very large truncation of the full shell-model space are necessary. We have allowed the following truncation: t_ν jumps from ($p_{3/2}$, $f_{5/2}$, $p_{1/2}$) to $g_{9/2}$, protons t_π jumps from $f_{7/2}$ to ($p_{3/2}$, $f_{5/2}$, $p_{1/2}$) orbital in each case. The calculation have been performed at SGI cluster computer at GANIL allowing highest feasible dimensions for each nucleus. Up to this dimension the states seem to be more convergen which can be taken as the final result. For ^{69}Cu, the ground state $3/2^-$ is well predicted by *fpga* interaction. The calculated $1/2^-$ and $5/2^-$ state is reverse in comparison to experimental levels. The calculated $1/2^-$ and $5/2^-$ state is at 134 KeV and at 378 KeV lower in energy from

the experimental levels. The order of $7/2^-_1$, $7/2^-_2$ and $9/2^-$ is well reproduced by this interaction. The $7/2^-_2$ is only 62 KeV below then experimental value. In ^{69}Cu the $3/2^-$ is interpreted by $\pi p_{3/2}$, the $5/2^-$ is interpreted by $\pi p_{5/2}$. The first $7/2^-$ is interpreted by $\pi p_{3/2} \otimes 2^+(^{68}\text{Ni})$ and the second $7/2^-$ is interpreted by $\pi p^{-1}_{7/2}$.

For ^{71}Cu, the ground state $3/2^-$ is well predicted by *fpg9a* interaction. The order of $5/2^-$ and $1/2^-$ state is reverse in comparison to experimental levels. The calculated $1/2^-$ level is 303 KeV higher than experimental value, while $5/2^-$ level is 179 KeV lower than the experimental result. The order of $7/2^-_1$, $7/2^-_2$ and $9/2^-$ is well reproduced and are higher in energy from the experimental values. In the ^{71}Cu, the $3/2^-$ is interpreted by $\pi p_{3/2}$, and the $5/2^-$ is interpreted by $\pi p_{5/2}$. The first $7/2^-$ is interpreted by $\pi p_{3/2} \otimes 2^+(^{70}\text{Ni})$ and the second $7/2^-$ is interpreted by $\pi p^{-1}_{7/2}$.

For ^{73}Cu, *fpg9a* interaction predicts $5/2^-$ state lower in energy by 15 KeV from $3/2^-$ state while experimentally $3/2^-$ is ground state. $1/2^-$ state is 462 KeV higher in energy from experimental value. The $9/2^-$ state lies in between two $7/2^-$ states. In the ^{73}Cu, the $3/2^-$ is interpreted by $\pi p_{3/2}$, and the $5/2^-$ is interpreted by $\pi p_{5/2}$. The first $7/2^-$ is interpreted by $\pi p_{3/2} \otimes 2^+(^{72}\text{Ni})$ and the second $7/2^-$ is interpreted by $\pi p^{-1}_{7/2}$.

Recently, there is experimental indication of $5/2^-$ as a ground state in ^{75}Cu at REX-ISOLDE, CERN [Fla09]. The *fpga* interaction also predicts $5/2^-$ as a ground state. For ^{77}Cu and ^{79}Cu, this interaction predicts $5/2^-$ as a ground state which is also expected from experiment. The calculations predict that the $1/2^-$, $9/2^-$ and $7/2^-$ states lie very high in energy for ^{79}Cu isotopes. The nickel isotopes (Z=28) cover three doubly-closed shells with number N=28, N=40, N=50 and therefore serve as a unique testing ground for large scale shell model calculations. Experimentally the 8^+ isomerism though expected to be present in a whole chain from ^{72}Ni to ^{76}Ni was found to be suddenly absent in ^{72}Ni and ^{74}Ni and present in ^{70}Ni and ^{76}Ni. The ground state spin from ^{68}Ni to ^{76}Ni is correctly reproduced by *fpg9a* interaction. For ^{70}Ni the first excited state 2^+ is calculated at 1.26 MeV which is 80 KeV below the experimental level. The states 4^+ at 2.68 MeV, 6^+ at 3.47 MeV, and 8^+ at 3.48 MeV are well predicted at 2.23 MeV, 2.68 MeV and 2.86 MeV. The agreement with the experimental data is excellent. For ^{72}Ni the first excited state 2^+ is calculated at 1.36 MeV which is 266 KeV above the experimental level. The states 4^+ at 1.94 MeV and 6^+ at 2.34 MeV are well predicted at 2.25 MeV and 2.47

MeV. Theoretically, there is 8^+ state at 2.62 MeV but experimentally there is no indication of 8^+ isomeric states. For ^{74}Ni only two excited states are experimentally known. The first excited state 2^+ is calculated at 1.56 MeV which is 533 KeV above the experimental value. The state 4^+ at 1.76 MeV is predicted at 2.32 MeV. The calculated 6^+, 8^+ states are at 2.57 MeV and 2.70 MeV respectively. For ^{76}Ni, the first calculated 2^+ state is slightly higher in energy about 557 KeV from the experimental value. The states 4^+ at 1.92 MeV, 6^+ at 2.28 MeV and isomeric states 8^+ at 2.42 MeV are well predicted at 2.17 MeV, 2.42 MeV and 2.53 MeV. The agreement for 4^+, 6^+ and 8^+ states with the experiment is excellent.

The ground state spin for $^{70-80}$Zn isotopes for $40 \leq N \leq 50$ is correctly reproduced by *fpga* interaction. For ^{70}Zn, the first excited 2^+ state is calculated at 0.603 MeV which is 282 KeV below the experimental value. The states 4^+ at 1.79 MeV, 6^+ at 2.89 MeV and 8^+ at 3.75 MeV are well predicted at 1.47 MeV, 2.37 MeV and 2.53 MeV. The calculated values are compressed in comparison to the experimental value. For ^{72}Zn, experimentally only 2^+ state at 0.653 MeV is known, which is predicted well by *fpga* interaction with energy difference of 74 KeV. The calculated values of states 4^+, 6^+ and 8^+ are at 1.178 MeV, 1.923 MeV and 2.601 MeV respectively. For ^{74}Zn, the first excited 2^+ state is calculated at 0.825 MeV which is 219 KeV above the experimental value. The states 4^+ at 1.419 MeV is predicted at 1.551 MeV. The states 6^+ and 8^+ are at 2.783 and 3.430 MeV. For ^{76}Zn, the first excited 2^+ state is calculated at 0.997 MeV which is 398 KeV above the experimental value. The first 4^+ state is calculated with energy difference of 679 KeV from the experimental value. The calculated 4^+, 6^+ and 8^+ states are at 1.975, 3.036 and 3.243 MeV respectively. For ^{78}Zn, the first excited 2^+ state is calculated at 1.307 MeV, which is 477 KeV above the experimental value. The states 4^+ at 1.621 MeV, 6^+ at 2.528 MeV and 8^+ at 2.673 MeV are predicted at 2.247 Mev, 2.923 MeV and 2.955 MeV. Experimentally, the difference between 6^+ and 8^+ states is 145 KeV while theoretically it is only 32 KeV. For ^{80}Zn the first excited 2^+ state is calculated at 1.953 MeV which is 461 KeV smaller than the experimental value.

The high values of $E(2_1^+)$ for Ni at N=40 is an indication of shell closure at N=40. For Zn isotopes the $E(2_1^+)$ and $E(4_1^+)$ at N=40 and 50 are high in comparison to neighbouring isotopes reflecting shell closure at N=40 and N=50. The calculated $B(E2;1/2^- \rightarrow 3/2^-)$ values show much better agrreement with experimental data compared to those earlier work of Stefanescu [Ste08]. The low B(E2) value beyond N=40 for $5/2^-$ state confirms its $\pi f_{5/2}$ single particle charactor. The sharp drop

in the excitation energy of $5/2^-$ state beyond N=40 could be due to the monopole migration. The large B(E2)value for $1/2^-$ state depart it from the single-particle charactor of $\pi p_{1/2}$ type.

The B(E2;$2_1^+ \rightarrow 0_{gs}^+$) value in ^{68}Ni is much lower as compared to ^{56}Ni. This low value was interprated by Sorlin *et al.* [Sor02] as orginating from the enhanced neutron pair scattering at $N = 40$ which is referred to as superfluid behaviour of the neutrons. The constancy of the B(E2) values beyond $N = 40$ can be understood as follows: *E2* strength as $np - nh$ excitation across $N = 40$ for odd n cannot contribute due to parity conservation and for even n are dominated by pair scattering. Langanke *et al.* [Lan03] performed microscopic calculations of the B(E2) in even-even nickel isotopes and found that the small observed B(E2) value is not necessarily an argument for a shell closure at N=40, but it simply reflects the fact that the lowest 2^+ state in ^{68}Ni is primarily a neutron excitation. Van de Walle *et al.* [Wal07] showed that B(E2) values in the Ni chain show a parabolic evolution between two magic numbers N=28 and 40 hinting a seniority-like behaviour . Peru *et al.* [Per06] measured high B(E2) value for ^{70}Ni at GANIL, and attributed it due to rapid proton core polarization when neutrons are added to the $g_{9/2}$ orbit.

The B(E2) value is almost constant from ^{68}Ni to ^{74}Ni and its value again decreases for ^{76}Ni. This decrease in B(E2) value is probably due to oncoming of the next shell closure at N=50 for ^{78}Ni. The experimental B(E2;$2_1^+ \rightarrow 0_{gs}^+$) values in the Zn isotopic chain show a similar trend towards $N = 40$ as the Ni isotopes up to ^{68}Zn, though for ^{70}Zn (at N = 40), the B(E2) value suddenly increases. Leesshardt *et al.* [Lee02] give three effects for supporting this increased collectivity: the addition of two protons out of the Ni core, the maximum in neutron pairing correlations at $N = 40$, and the presence of the strongly downsloping $l = 4$ Nilsson neutron orbitals close to the Fermi surface. Kenn *et al.* [Ken02] indicate that the inclusion of the $g_{9/2}$ orbit in the valence space is important in order to reproduce the increased B(E2;$2_1^+ \rightarrow 0_{gs}^+$) values in the ^{70}Zn.

The calculated B(E2;$2_1^+ \rightarrow 0_{gs}^+$) values in present work obtained using *fpg9a* interaction for $^{70-80}$Zn show similar trends as experimental values from ^{70}Zn to ^{80}Zn. The B(E2) value at N=50 is very low, this is an indication of shell closure at N=50. These results indicate that further modification in interaction and inclusion of $1d_{5/2}$ orbit is important in the shell model calculations.

In **Chapter 8**, summary of the present work is given and future prospects are discussed. The present work can be extended to the study of following aspects:

1. the role of $d_{5/2}$ orbital from *sdg* shell in the evolution of shell structure towards ^{78}Ni.

2. the role of tensor part of the proton-neutron interaction, especially between the proton *fp* and neutron $g_{9/2}$ orbital.

3. the role of particle-hole excitations through Z=28 and N=40 shell gaps for the onset of deformation below and above ^{68}Ni.

4. shell evolution around the ^{100}Sn and ^{132}Sn doubly magic nuclei. Further, to study the structure of Sn isotopes above ^{132}Sn and new shell closure at ^{140}Sn in the context of r-process.

5. the role of shell structures and deformation in Pb region.

Bibliography

[Bec05] E. Becheva *et al.*, Phys. Rev. Lett. **84** (2005), 5493.

[Ber90] M. Bernas *et al.*, Z. Phys. A **41** (1990), 336.

[Bro01] B.A. Brown *et al.*, Prog. Part. Nucl. Phys. **47** (2001), 517.

[Cau89] E. Caurier, *code ANTOINE*, Strasbourg, 1989.

[Cau99] E. Caurier and F. Nowacki, Acta Phys. Pol. B **30** (1999), 705.

[Dea99] D.J. Dean *et al.*, Phys. Rev. C **59** (1999), 2474.

[Dob08] J.J. Valiente Dobón *et al.*, Phys. Rev. C **78** (2008), 024302.

[Duf96] M. Dufour *et al.*, Phys. Rev. C **54** (1996), 1641.

[Fla09] K. T. Flanagan *et al.*, Phys. Rev. Lett. **103** (2009), 142501.

[Fra01] S. Franchoo *et al.*, Phys. Rev. C **64** (2001), 054308.

[Hau88] P. E. Haustein *et al.*, At. Data and Nuclear tables **39** (1988), 185.

[Hey94] K. Heyde, *The Nuclear Shell Model, Study Edition*, Springer-Verlag, Berlin, 1994.

[Hon04] M. Honma *et al.*, Phys. Rev. C **69** (2004), 034335.

[Jen95] M. H. Jensen *et al.*, Phy. Rep. **261** (1995), 125.

[Kah69] S. Kahana *et al.*, Phys. Rev. **180** (1969), 956.

[Ken02] O. Kenn *et al.*, Phys. Rev. C **65** (2002), 034308.

[Kuo67] T.T.S. *et al.*, Nucl. Phys. A **103** (1967), 71.

[Lan03] K. Langanke *et al.*, Phys. Rev. C **67** (2003), 044314.

[Law80] R. D. Lawson *Theory of Nuclear Shell Model*, Calarendon Press, Oxford, 1980.

[Lee02] S. Leenhardt *et al.*, Eur. Phys. Jour. A **14** (2002), 1.

[Lid06] S.N. Liddick *et al.*, Phys. Rev. C **73** (2006), 044322.

[Lis04] A. Lisetski *et al.*, Phys. Rev. C **69** (2004), 044314.

[Lur07] S. Lurandi *et al.*, Phys. Rev. C **76** (2007), 034303.

[Mic06] S. Michimasa *et al.*, Phys. Lett. B **638** (2006), 160.

[Now96] F. Nowacki Ph.D. thesis, IRes, Srasbourg, 1996.

[NNDC] Data extracted using the NNDC World Wide Web site from the ENSDF.

[Ots99] T. Otsuka *et al.*, Phys. Rep. **264** (1999), 297.

[Oza05] A. Ozawa *et al.*, Phys. Rev. Lett. **84** (2005), 5493.

[Per06] 0. Perru *et al.*, Phys. Rev. Lett. **96** (2006), 232501.

[Pov01] A. Poves *et al.*, Nucl. Phys. A **403** (2001), 213.

[Pre72] B.M. Preedom *et al.*, Phys. Rev. C **6** (1972), 1633.

[Ren95] Z. Ren *et al.*, Phys. Rev. C **52** (1995), R 20.

[Sak99] H. Sakurai *et al.*, Phys. Lett. B **448** (1999), 180.

[Sha63] A. de Shalit *Nuclear Shell Theory*, Academic Press, New York, 1963.

[She96] Y.S. Shen *et al.*, Z. Phys. A **356** (1996), 133.

[Smi04] N. Smirnova *et al.*, Phys. Rev. C **70** (2004), 044306.

[Sor02] O. Sorlin *et al.*, Phys. Rev. Lett. **88** (2002), 092501.

[Ste08] I. Stefanescu *et al.*, Phys. Rev. Lett. **100** (2008), 112502.

[Wal07] J. Van de Walle *et al.*, Phys. Rev. Lett. **99** (2007), 142501.

[War90] E. K. Warburton *et al.*, Phys. Rev. C **41** (1990), 1147.

[Wil71] B. H. Wildenthal *et al.*, Phys. Rev. C **4** (1971), 1708.